



ORIGINAL RESEARCH ARTICLE

Resistance Rivet Welding of Aluminum Alloy and Steel with a Supplementary Plate

Hongxin Shi, Shibo Zhu, Yanling Hu, Han Guo, Xiao Xiao, and Ranfeng Qiu

Submitted: 30 October 2023 / Revised: 2 December 2023 / Accepted: 29 December 2023

A combination of self-pierce riveting and resistance spot welding, which is named resistance rivet-welding, was used to join aluminum alloy sheet and mild steel sheet. To enhance the performance of the joints between aluminum alloy and mild steel, a supplementary plate was used for joining. The effect of welding current on the performance and cross-section geometrical characteristics of resistance rivet-welded joints with and without supplementary plate was compared and analyzed. A reaction layer composed of Fe_2Al_5 and FeAl_3 was formed at the interface between the rivet leg and the aluminum alloy, the mild steel and aluminum alloy in the resistance rivet-welded joint with supplementary plate. The tensile shear load and cross tension load of resistance rivet-welded joint with supplementary plate increased first and then decreased with the increase in welding current, which achieved the maximum value of 7.51 kN and 4.23 kN when the welding current was 6 kA, respectively. The results reveal that the application of supplementary plate in the resistance rivet-welding between the aluminum alloy and mild steel can not only prevent the failure of the rivet cap being pulled out from the upper plate when the joint is loaded, but also improve the tensile shear load and cross tension load of the joint.

Keywords aluminum alloy, mild steel, resistance rivet-welding

1. Introduction

In the last ten years, the resistance spot welding between aluminum alloy and steel has been widely concerned to realize the lightweight of automobile body and develop low-carbon economy (Ref 1). It is troublesome to directly perform RSW for AA and steel due to the melting of part of the base material during welding. This is because the two materials of AA and steel have large differences in melting point and resistivity, and brittle intermetallic compounds are easily form at the welding interface between AA and steel (Ref 2-4). In view of this, the RSW of AA and steel has been widely studied in order to improve the interfacial microstructure and enhance the performance of the joint.

Improving the welding temperature field by physical means to control the interfacial microstructure and improve the joint performance is one of the many researches on the resistance

spot welding of aluminum alloy and steel. Applying a cover plate of steel on aluminum alloy side to balance the temperature field on both sides of aluminum alloy plate and steel during resistance spot welding can prevent the skew of nugget, and then, the performance of resistance spot welded joint of aluminum alloy and steel was improved (Ref 5-7). The development of delta spot welding process made the applying of cover plate realize mechanization, improved the efficiency of the technology, and provided a guarantee for the engineering application of the technology (Ref 8, 9). An electrode tip with small diameter was used on the aluminum alloy side to increase the current density and improve the temperature field during resistance spot welding of aluminum alloy and steel, by which the performance of the resistance spot welded joint between aluminum alloy and steel can also be enhanced without the application of additional auxiliary materials (Ref 10). However, the interfacial reaction layer is still the main factor restricting the further improvement the performance of resistance spot welded joint of aluminum alloy and steel, although the tensile shear load (TSL) of the joint can be increased to a certain extent using such physical means to regulate the temperature field (Ref 11).

It is another important branch of the study on the resistance spot welding of aluminum alloy and steel to improve the interfacial microstructure and performance of the joint regulating the metallurgical reaction between aluminum alloy and steel at the welding interface by using chemical method. Some materials, such as Zn (Ref 12, 13), Cu (Ref 14), A1050 (Ref 15), Al-Si brazing filler metal (Ref 16, 17), were selected as the intermediate transition layer in resistance spot welding of aluminum alloy and steel according to their metallurgical characteristics. It can be seen from the results that the application of the intermediate layer only inhibited the growth of the interfacial reaction layer to a certain extent, or changed the composition of the interfacial reaction layer, and that the

Hongxin Shi, Xiao Xiao, and Ranfeng Qiu, School of Materials Science and Engineering, Henan University of Science and Technology, Luoyang 471039, China; and Provincial and Ministerial Co-construction of Collaborative Innovation Center for Nonferrous Metal New Materials and Advanced Processing Technology, Luoyang 471039, China; **Shibo Zhu**, School of Materials Science and Engineering, Henan University of Science and Technology, Luoyang 471039, China; **Yanling Hu**, Library, Henan University of Science and Technology, Luoyang 471039, China; and **Han Guo**, Office of Science and Technology, Henan University of Science and Technology, Luoyang 471039, China. Contact e-mail: qieurfl221@163.com.

adverse effect of interfacial reaction layer on the performance of resistance spot welded joint of aluminum alloy and steel has not been eliminated.

Under the background, the study on changing the structure of resistance spot welded joint of aluminum alloy and steel by introducing an element of steel whose axis is perpendicular to the welding interface into the joint has attracted wide attention. In order to obtain a sounder joint, a variety of rivets, such as cylinder headless rivet (Ref 18), circular table headless rivet (Ref 19), flat head rivet (Ref 20-23), countersunk rivet (Ref 24), semi-tubular rivet (Ref 25, 26), conical rivet (Ref 27, 28), were selected as the element for the resistance spot welding of aluminum alloy and steel. A key point of the technique is that the rivet of element passes through the upper sheet of aluminum alloy and is joined with the lower plate of steel. Therefore, various methods of introducing the element have been tried to explore the reliability of the process and simplify it. The most traditional method of introducing the element is to premachine a hole in the upper sheet of aluminum alloy and press the rivet into the prefabricated hole so that the end of the rivet leg is in contact with the lower sheet of steel, then align the electrode with the rivet for resistance spot welding to form a joint (Ref 18-26). In order to simplify the manufacturing process, drilling hole and rivet introduction were combined into one process in some studies (Ref 29, 30). Oliveira et al. used the combining method of friction element welding and resistance spot welding to join aluminum alloy and high strength steel, in which the element was introduced into the joint by friction element welding (Ref 31). On this basis, the leg of element was processed more sharply and was directly pressed through the upper sheet of aluminum alloy by using electrode force in the absence of prefabricated hole, and then, resistance spot welding was carried out in situ (Ref 26-28).

Self-pierce riveting (SPR) is a solid-state joining method and is suitable for joining of dissimilar material. In terms of equipment, resistance spot welding and SPR have certain similarities and great potential for compatibility. On account of this, a combining method of SPR and resistance spot welding (the method is henceforth called resistance rivet-welding, RRW) was put forward for joining aluminum alloy and steel to overcome the technical limitations of considerably unequal sheet thickness combination on the SPR of aluminum alloy and steel, in which the element was introduced into the joint by SPR (Ref 32). However, the failure of the aluminum alloy and steel RRW joint was mainly in the form of the rivet cap being pulled out from the upper sheet of aluminum alloy (Ref 33).

Therefore, to further enhance the performance of RRW joints between aluminum alloy and steel, it is necessary to use wide shoulder rivet for joining. As a preliminary study, a supplementary plate (SP) of steel was placed on the aluminum alloy sheet and then RRW was performed to expand the rivet shoulder area, which provides support for the design of wide shoulder rivet in the future.

2. Experimental Materials and Procedures

The materials included 2.00-mm-thick Q235 mild steel sheet and A5052 aluminum alloy sheet. The nominal compositions are listed in Table 1. The sheets were cut at a size of 100 mm × 30 mm. A 30 mm × 30 mm × 1.0 mm Q235 mild steel sheet was used as a SP. The rivets of selected for

this experiment are SWCH35K rivets with a shank diameter of 5.3 mm. Here, the length of the rivet was selected according to the thickness of the sheets to be joined (Ref 34). After washing with anhydrous ethanol and drying, A5052 aluminum alloy sheet, Q235 mild steel sheet and SP were assembled to the specimens as shown in Fig. 2(a) and (b), which were used for tensile shear and cross tension testing, respectively.

The process of RRW includes two stages of SPR and resistance spot welding. When SPR was implemented, the aluminum alloy sheet and mild steel sheet were selected as the upper plate and the lower plate, respectively. The SP was placed on the aluminum alloy sheet as shown in Fig. 1. The SPR pressure was changed every 2 kN within the range of 16-28 kN under the condition that the feeding time was 1 s and the return time was 0.5 s. The joint obtained at this stage was called a SPR joint. The TSL and cross tension load (CTL) of SPR joints were tested at room temperature under a cross-head velocity of 1.7×10^{-5} m/s. The optimum riveting pressure was selected according to the TSL and CTL values of SPR joint. In the resistance spot welding stage, the electrodes were aligned with the rivet in the SPR joint obtained under optimum riveting pressure conditions for welding. Welding was implemented on the projection using a stationary DC spot welding machine. Electrodes with a tip diameter of 6 mm were used. The welding current was changed every 2 kA in the range of 4-12 kA keeping welding time at 20 cycles, squeezing time at 10 cycles, holding time at 10 cycles and electrode force at 3 kN constant during resistance spot welding. The joint obtained in the case was called a RRW joint. Similarly, the TSL and CTL of RRW joints were also tested. For each joining condition, 5 samples using tensile shear test, 5 samples using cross tension test and 2 samples using cross-section observation were welded.

The SPR and RRW joints were cut perpendicular to the faying surface through the rivet center, and a cross-section observation experiment was conducted after grinding and polishing. The microstructure of RRW joints was investigated by scanning electron microscopy (SEM), and the chemical compositions of the reaction products were assessed by energy-dispersive x-ray spectroscopy (EDS).

For comparison, the SPR and RRW joints without SP were also manufactured under the same conditions as those SPR and RRW joints with SP, respectively.

3. Experimental Results and Discussion

Figure 2(a) and (b) displays the optical micrograph of SPR joint cross-sections joined at the riveting pressure of 24 kN without and with SP, respectively. Although a mechanical lock between the rivet and the lower plate was observed in the two types of joints, there were some differences in their geometric characteristics. First, a gap pointed by an arrow at the J position (Fig. 2(b)) was observed between the outer edge of the rivet cap and the SP in the SPR joint with SP. This is because aluminum alloy is more prone to plastic deformation than steel under the same pressure. In the case of SPR without SP, the rivet cap was in close contact with the A5052 of the upper plate, and then, it was embedded in the A5052 due to the plastic deformation of aluminum alloy under the action of riveting pressure. However, the rivet cap was in contact with the SP under riveting pressure in the case of SPR with SP. After the release of riveting pressure, the rivet cap had a certain degree of springback due to

Table 1 Chemical compositions of A5052 and Q235 steel (wt.%)

Material	Cu	Mg	V	C	P	S	Zn	Cr	Si	Mn	Fe	Al
A5052 AA	0.10	2.5	0.10	0.25	0.25	0.10	0.40	Bal.
Q235 MS	0.06	0.14	0.04	0.02	0.4	1	Bal.	—

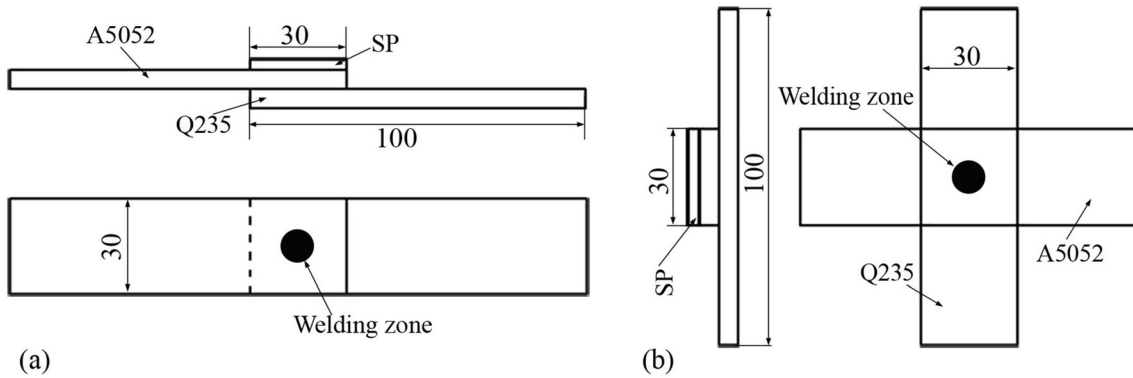


Fig. 1 Assembly diagram of sample to weld (a) using tensile shear test; (b) using cross tension test

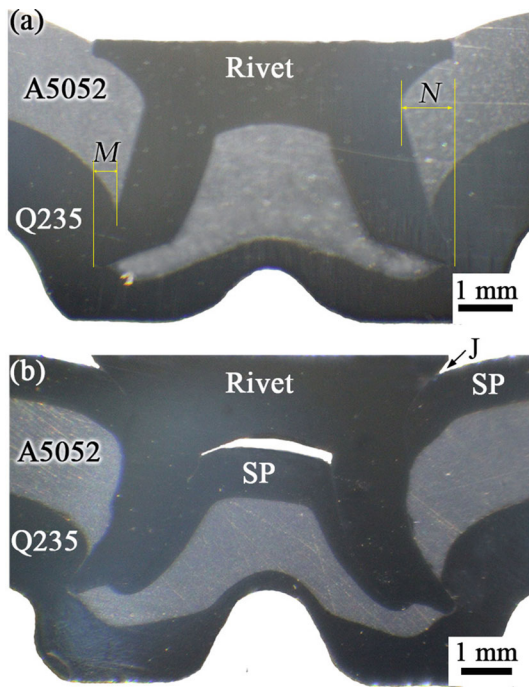


Fig. 2 Macrographs of cross-sectional joints (a) SPR joint without SP; (b) SPR joint with SP

the little plastic deformation of the SP. Under the amplification action of the lever, the gap was formed between the rivet cap edge and the SP as shown in Fig. 2(b).

Second, there is also a gap between the SP and the rivet cap inside rivet skirt of SPR joint with SP as shown in Fig. 2(b). This is because of the larger friction force between the rivet leg and the SP during SPR. Compared with the SPR without SP, the transverse force of the rivet leg on the SP was larger in the

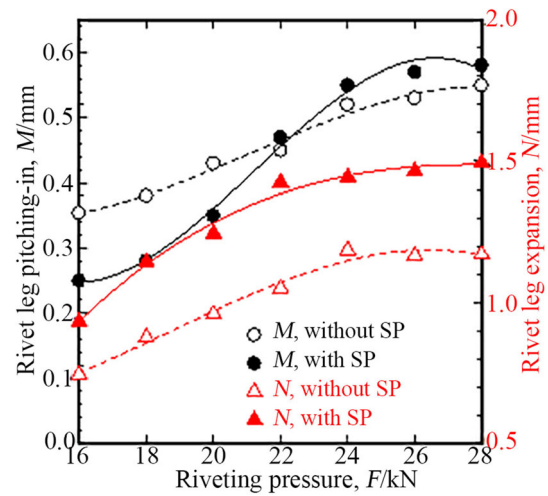


Fig. 3 Effects of riveting pressure on the rivet leg pitching-in and expansion of the SPR joints

case of SPR with SP under the condition that the leg diameter of the rivet and the shape of the SPR die were the same because there was an extra layer of SP inside the rivet skirt. This resulted in a larger friction force between the rivet leg and the SP, and the SP was pushed into the aluminum alloy under the action of the friction force, so that it was separated from the rivet cap and the gap was formed. The experiment results also showed that the smaller the riveting pressure, the larger the gap width.

For the two types of SPR joints, the cross-section geometrical parameters of the joint were also affected by the riveting pressure. Rivet leg expansion (N) and pitching-in (M) are the main parameters that affect the SPR joint performance. Figure 3 displays the effects of riveting pressure on the rivet leg expansion and pitching-in of the SPR joints. For both types of

SPR joints, the rivet leg expansion increased with the increase in the riveting pressure. Under the same riveting pressure, the rivet leg expansion of the SPR joint with SP was larger than that of the SPR joint without SP. This is because the rivet leg was subjected to greater outward force during SPR with SP as previously mentioned.

For the SPR joints without SP, the rivet leg pitching-in increased gently with the increase in the riveting pressure. In the case of SPR joints with SP, the rivet leg pitching-in increased with the increase in the riveting pressure in range of 16-24 kN, whereas it tended to be relatively stable when the riveting pressure was greater than 24 kN. In range of 16-22 kN, the rivet leg pitching-in of SPR joint without SP was larger than that of the SPR joint with SP fabricated under the same riveting pressure. However, the relationship was reversed when the riveting pressure was greater than 22 kN. As shown in Fig. 2, the rivet leg pitching-in refers to the transverse length of the rivet leg into the lower plate after penetrating the upper plate. The application of the SP increased the resistance of the rivet during the SPR. In the lower rivet pressure range (16-22 kN), the length of the rivet leg through the upper plate in the SPR joint with SP was less than that in the SPR joint without SP fabricated under the same riveting pressure. This is considered to be the reason why the rivet leg pitching-in of the joint with SP was less than that of the joint without SP in the riveting pressure range. When the riveting pressure was larger, the rivet leg penetrated the A5052 of the upper plate more fully for the two types of SPR joints. Meanwhile, the rivet leg bore larger outward force during SPR with SP in comparison with the SPR without SP as mentioned above. This resulted in rivet leg pitching-in of the SPR joint with SP larger than that of the SPR joint without SP when the riveting force was greater than 22 kN.

Figure 4 shows the effects of riveting pressure on the TSL and CTL of the joints. For the SPR joint without SP, the TSL and CTL of joints increased first and then decreased with the increase in riveting pressure. When the riveting pressure was 24 kN, they reached the maximum value of 5.83 kN and 2.58 kN, respectively. The larger the riveting pressure, the larger the rivet leg expansion and pitching-in. This is the reason why the TSL and CTL of joint without SP increased with the

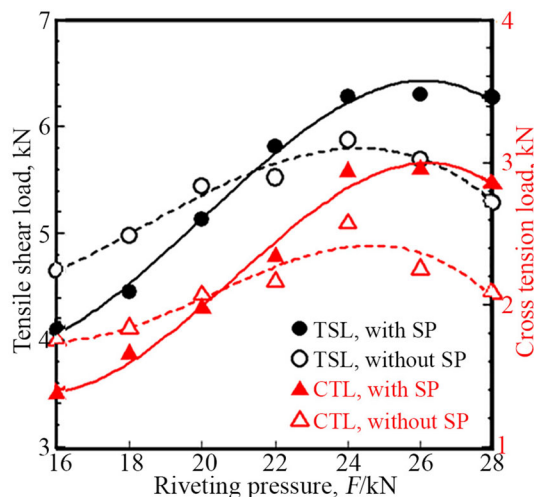


Fig. 4 Effects of riveting pressure on the TSL and CTL of the SPR joints

increase in riveting pressure in the range of 16-24 kN. However, the rivet cap was pressed into the A5052 of the upper plate when the riveting pressure was higher. This resulted in the TSL and CTL of the SPR joint without SP decreased with increasing riveting pressure when the riveting pressure was larger than 24 kN. In the case, the rivet cap was pulled out from the upper plate during the tensile shear and cross tension tests, which caused the joint to break and failure. In the case of SPR joint with SP, with increasing riveting pressure, the TSL and CTL of joints increased in the riveting pressure range of 16-24 kN and then remained relatively stable above the riveting pressure of 24 kN, approximately 6.29 kN and 2.94 kN, respectively. This is thought to be the result of the influence of the rivet leg expansion and pitching-in, because their dimensions (especially the latter) represent the size of the mechanical interlock formed in the joint.

Comparing the performance variation curves of the two types of joints as shown in Fig. 4, some differences can be found. First, the gradients of TSL and CTL of SPR joints with SP were larger than those of the SPR joint without SP in the riveting pressure range of 16-24 kN. This also resulted in that the TSL and CTL of the SPR joint with SP exceed that of the SPR joint without SP when the riveting pressure was greater than 22 kN, respectively. This should be attributed to the fact that the rivet leg pitching-in of the SPR joint with SP increased rapidly with the increase in riveting pressure as shown in Fig. 3. Second, with increasing riveting pressure, the TSL and CTL of joints with SP remained stable, whereas those of joints without SP decreased when the riveting pressure was larger than 24 kN. This is also due to the application of SP. Although the rivet leg expansion and pitching-in remained relatively stable for both types of joints with and without SP when the riveting pressure was greater than 26 kN, the rivet cap was pressed into the A5052 of the upper plate in the SPR joint without SP due to excessive riveting pressure, which caused the joint performance to decline. However, the application of the SP avoided this phenomenon in the SPR with SP. This is because the SP was not easy to plastic deformation under the action of riveting pressure, and its application increased the area of the aluminum alloy subjected to the pressure of the rivet shoulder. From the above results, it can be concluded that the higher riveting pressure should be selected when the SP is used for the SPR of A5052 and Q235 mild steel.

According to the TSL and CTL of the joints in the study, the SPR joint obtained at the riveting pressure of 24 kN was selected for subsequent resistance spot welding to obtain RRW joints. Figure 5(a) and (b) displays the cross-sections optical micrograph of RRW joint without and with SP, respectively. The joints were welded at a welding current of 8 kA. It can be seen from Fig. 5 that they inherit the characteristics of the joint obtained in the previous stage of SPR in terms of the cross-section macroscopic morphology of the joint. However, the rivet cap and the SP were pressed tightly, and no gap was observed between them in the RRW joint with SP. This shows that pressurizing and heating the SPR joint is conducive to the formation of reliable joint.

Figure 6 displays the effects of welding current on the rivet leg expansion and pitching-in of the RRW joints. Here, solid blue line and solid green line represent the rivet leg pitching-in and expansion of the SPR joint with SP manufactured at the riveting pressure of 24 kN, respectively. Blue dotted line and green dotted line show those of the SPR joint without SP obtained at the riveting pressure of 24 kN, respectively. As

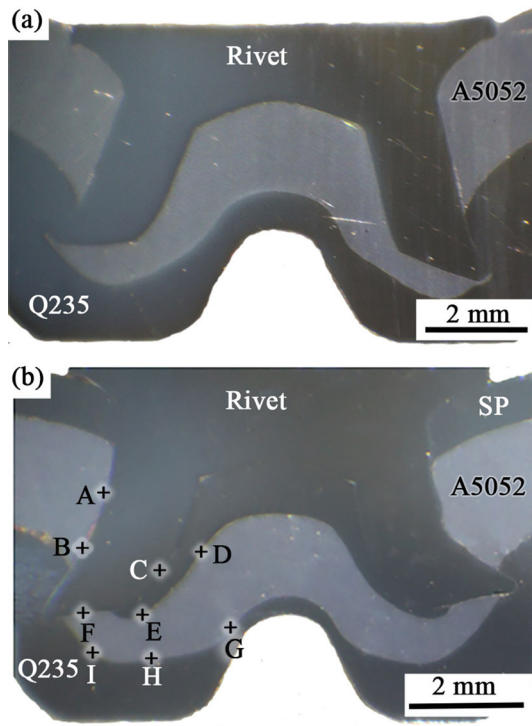


Fig. 5 Macrographs of cross-sectional joints (a) RRW joint without SP; (b) RRW joint with SP

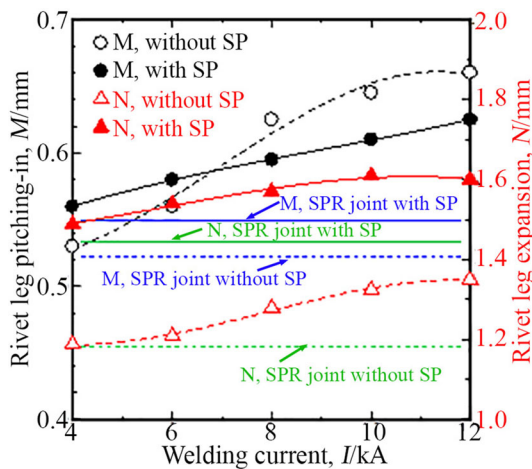


Fig. 6 Effects of welding current on the rivet leg pitching-in and expansion of the RRW joints

shown, regardless of the welding current used, the rivet leg pitching-in and expansion of the RRW joints with and without SP were larger than those of the SPR joint with and without SP, respectively. For the two types of RRW joints, the rivet leg expansion and pitching-in increased with the increase in welding current. However, the increase rates of rivet leg pitching-in and expansion of RRW joints without SP were larger than those of the RRW joint with SP. As a result, when the welding current was greater than 8 kA, the rivet leg pitching-in of RRW joint without SP was larger than that of RRW joint with SP welded under the same welding current. On the other hand, the rivet leg expansion of the RRW joint with SP was larger than that of the RRW joint without SP in the

range of welding current used as shown in Fig. 6. This is due to the large difference in the rivet leg expansion between the SPR joints with and without SP. Although the rivet leg expansion of the RRW joint without SP increased rapidly with the increase in welding current, it still failed to exceed that of the RRW joint with SP welded the same welding current. The SPR joint was heated and pressurized in the RSW stage, which caused the joint to undergo plastic deformation under the action of electrode force. For the RRW joints with and without SP, this is the reason why the rivet leg expansion and pitching-in were larger than those of the SPR joints with and without SP, respectively. However, the presence of SP inside the rivet skirt of SPR joint with SP increased the resistance of the joint against plastic deformation. As a result, the rivet leg expansion and pitching-in of RRW joints with SP increased more slowly with the increase in welding current in comparison with the RRW joints without SP.

Figure 7 shows the SEM images of various interfaces in the RRW joint with SP, in which Fig. 7 (a), (b), (c), (d), (e), (f), (g), (h) and (i) is taken from the locations of A ~ I in Fig. 5, respectively. A reaction layer was observed at the interface between the rivet leg and the upper plate A5052 (outside the rivet leg) as shown in Fig. 7(a) and (b). The observation results show that the reaction layer formed near the end of the rivet leg was thicker. Similarly, a reaction layer was also observed at the interface between the rivet leg (or SP) and the upper plate A5052 inside the rivet skirt as shown in Fig. 7(d), (e) and (f). In this case, the closer to the end of rivet leg, the thicker the reaction layer formed. The reaction layer formed at the location of F in Fig. 5 was approximately 5.0 μm thick as shown in Fig. 7(f). There is also a reaction layer formed at the interface between the lower plate steel and the upper plate A5052 below the rivet skirt as shown in Fig. 7(g), (h) and (i). As the distance to the axial line of the rivet is closer, its thickness is smaller. The thickness of the reaction layer at the interface below the end of the rivet leg was also approximately 5.0 μm as shown in Fig. 7(i). The formation of reaction layers at the dissimilar material interfaces in the RRW joint (such as the interface between the upper plate A5052 and the rivet leg, A5052 and SP, A5052 and the lower plate steel) indicates that the implementation of resistance spot welding for the SPR joint can produce metallurgical joining at these interfaces in the joint. As shown in Fig. 7, the thickness of the reaction layer varied with the position at each interface in the RRW joint with SP. In general, the reaction layer formed closer to the end of the rivet leg was thicker. During resistance spot welding for the SPR joint, the welding current flowed from the rivet cap to the lower plate steel along the rivet leg in the SPR joint. Due to the contact resistance between the end of the rivet leg and the lower plate steel, more Joule heat was precipitated here. This caused a thicker reaction layer to form at the dissimilar material interfaces near the rivet leg end, because of the higher temperature and longer high-temperature duration there. As shown in Fig. 7 (c), additionally, there was also a good bonding between the rivet and the SP under the action of heat and force during resistance spot welding.

In terms of morphology, the reaction layers adjacent to steel (the Q235 steel, SP or rivet leg) demonstrated a larger undulating state, whereas those adjacent to the aluminum alloy showed relatively smooth morphology as shown in Fig. 7. The compositional analysis for the interfacial reaction layers was performed, and the results are shown in Table 2. The results manifested that the chemical composition at the Q_1 , Q_2 and Q_3

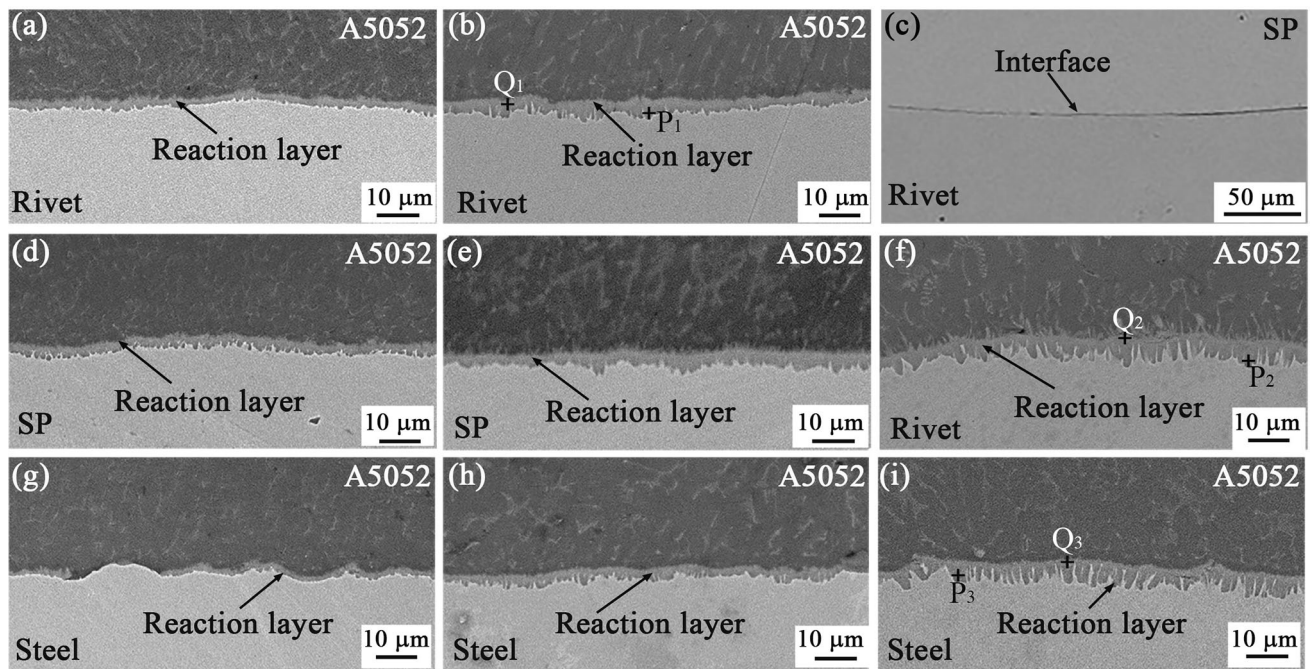


Fig. 7 SEM images of various interfaces in the RRW joint without SP (a), (b), (c), (d), (e), (f), (g), (h) and (i) taken from the locations of $A \sim I$ in Fig. 5, respectively

Table 2 EDS results (at.%)

Elements	P_1	P_2	P_3	Q_1	Q_2	Q_3
Fe	29.59	27.70	28.72	23.52	23.84	24.62
Al	70.41	72.30	71.28	76.48	76.16	75.38

locations adjacent to the aluminum alloy was consistent with the nominal stoichiometry of Fe_2Al_5 , while composition at the P_1 , P_2 and P_3 locations adjacent to steel was in accord with one of $FeAl_3$. Therefore, the reaction layers formed in the RRW joint with SP were composed of Fe_2Al_5 and $FeAl_3$. The morphology and composition of the reaction layers in the RRW joint with SP are consistent with those of resistance spot welded Al/steel joints welded by using other technological measures (Ref 10, 25, 35). The reasons for these have been reported in detail (Ref 6).

Figure 8 shows the effects of welding current on the TSL and CTL of the RRW joints. Here, solid blue line and solid green line represent the TSL and CTL of the SPR joint with SP manufactured at the riveting pressure of 24 kN, respectively. Blue dotted line and green dotted line show those of the SPR joint without SP obtained at the riveting pressure of 24 kN, respectively. For the two types of RRW joint, the TSL and CTL of joints increased first and then decreased with the increase in welding current. When the welding current was 6 kA, the TSL and CTL of the RRW joint with SP achieved the maximum value of 7.51 kN and 4.23 kN, respectively. In the case of RRW without SP, the maximum TSL and CTL of the joint were 6.60 kN and 3.28 kN when the welding current was 8 kA, respectively. In terms of the maximum load obtained in this

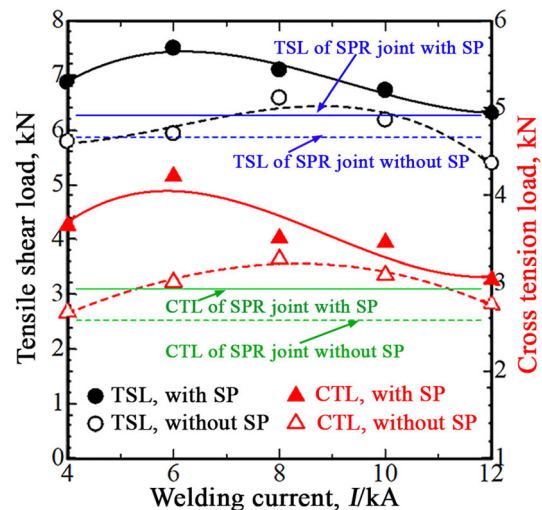


Fig. 8 Effects of welding current on the TSL and CTL of the RRW joints

study, the TSL and CTL of the RRW joint with SP were improved by 13.8% and 29.0% compared to those of RRW joint without SP, respectively. Compared with the TSL and CTL of SPR joint with SP, those of RRW joints with SP were larger in the welding current range of 4-12 kA as shown in Fig. 8. In the case without SP, the CTL of RRW joints was larger than that of the SPR joint, whereas the TSL of the RRW joints was larger than that of the SPR joint in the welding current range of 4-10 kA, and the relationship was reversed when the welding current was larger than 12 kA.

For tensile shear and cross tension testing, the failure modes of RRW joints with SP had two forms of rivet leg fracture and rivet leg pulled out. The failure mode of RRW joint with SP was the rivet leg fracture when the welding current was less than 6 kA, whereas one of the RRW joint was rivet leg pulled out when welding current exceeded 6 kA. In the case without SP, the failure modes of RRW joints mainly included rivet leg fracture and rivet cap pulled out whether tensile shear test or cross tensile test. The failure mode of RRW joint without SP was the rivet leg fracture when the welding current was less than 8 kA, whereas one of the RRW joint was rivet cap pulled out when welding current exceeded 8 kA.

With the increase in welding current, more heat is generated during resistance spot welding, which makes the metallurgical bonding between the rivet leg and the surrounding metal more adequate in the joint. Therefore, the CTL and TSL of the RRW joints with and without SP increased with increasing welding current in the lower welding current range. However, excessive welding current can cause a thick reaction layer to form at the interface between the rivet leg and the upper plate A5052. Hence, the interfaces between the rivet leg and the upper plate A5052 in the RRW joints with SP were damaged under the action of load, which resulted in the rivet leg being pulled out and then caused the joint failure. As a result, the CTL and TSL of the RRW joints with SP decreased with the increase in welding current when it exceeded 6 kA. In addition, excessive welding current can also cause the rivet cap to sink deeper into the upper plate A5052 in the RRW joints without SP, which caused the rivet cap to pull out from the upper plate A5052 under the action of load, then resulted in the failure of the joint. Consequently, the CTL and TSL of the RRW joints without SP decreased with the increase in welding current when it exceeded 8 kA. It should be noted from Fig. 8 that the welding current required for the maximum TSL and CTL of the RRW joint with SP was lower than that of the RRW joint without SP. This is considered to be due to the fact that the resistance of the joint with SP is greater than that of the joint without SP because of the presence of SP in the joint. The results show that the application of SP in the RRW between the aluminum alloy and mild steel can not only prevent the failure of the rivet cap being pulled out from the upper plate when the joint is loaded, but also improve the TSL and CTL of the joint.

4. Conclusions

The following conclusions can be drawn from the comparative analysis of the sectional characteristics and performance of the two types of RRW joints with and without SP:

1. The rivet leg pitching-in and expansion in the RRW joint with SP increased with the increase in welding current.

2. A reaction layer composed of Fe_2Al_5 and FeAl_3 was formed at the interface between the rivet leg and aluminum alloy, the steel and aluminum alloy in the RRW joint with SP.

3. The TSL and CTL of RRW joint with SP increased first and then decreased with the increase in welding current, which achieved the maximum value of 7.51 kN and 4.23 kN when the welding current was 6 kA, respectively.

4. The maximum TSL and CTL of the RRW joint with SP were improved by 13.8% and 29.0% compared to those of RRW joint without SP, respectively.

5. Widening the rivet shoulder can strengthen the performance of RRW joint between aluminum alloy and steel.

Acknowledgments

The authors would like to express their gratitude to the Frontier Exploration Project from Longmen Laboratory of Henan Province, China (Grant No. LMQYTSKT010 and LMQYTSKT004) for financial support.

Conflict of interest

No potential conflict of interest was reported by the author(s).

References

1. A.S. Imtiaz, R.P. Srinivasa, and A. Mokhtar, A Review of Advances in Resistance Spot Welding of Automotive Sheet Steels: Emerging Methods to Improve Joint Mechanical Performance, *Int. J. Adv. Manuf. Technol.*, 2022, **118**, p 1335–1366
2. K. Ren, R. Qiu, H. Ma, and H. Shi, Joining Aluminum Alloy to Steel by Resistance Projection-Plug Welding, *J. Mater. Eng. Perform.*, 2020, **29**(6), p 4087–4094
3. A. Gullino, P. Matteis, and F. D’Aiuto, Review of Aluminum-to-Steel Welding Technologies for Car-Body Applications, *Metals*, 2019, **9**, p 315
4. Y. Zhang and D. Sun, Microstructures and Mechanical Properties of Steel/Aluminum Alloy Joints Welded by Resistance Spot Welding, *J. Mater. Eng. Perform.*, 2017, **26**(6), p 2649–2662
5. S. Satonaka, C. Iwamoto, R. Qiu, and T. Fujioka, Trends and New Applications of Spot Welding for Aluminum Alloy Sheets, *Weld. Int.*, 2006, **20**(11), p 858–864
6. R. Qiu, C. Iwamoto, and S. Satonaka, Interfacial Microstructure and Strength of Steel/Aluminum Alloy Joints Welded by Resistance Spot Welding with Cover Plate, *J. Mater. Process. Technol.*, 2009, **209**, p 4186–4193
7. R. Qiu, H. Shi, H. Yu, and K. Zhang, Joining Phenomena of Stainless Steel/Aluminium Alloy Joint Welded by Thermal Compensation Resistance Spot Welding, *Int. J. Mater. Prod. Technol.*, 2014, **49**(4), p 285–293
8. J.S. Kim, I.J. Kim, and Y.G. Kim, Optimization of Welding Current Waveform for Dissimilar Material with DP590 and Al5052 by Delta-Spot Welding Process, *J. Mech. Sci. Technol.*, 2016, **30**(6), p 2713–2721
9. Y. Che, L. Wang, D. Sun, H. Li, and W. Geng, Microstructures and Mechanical Properties of Resistance Spot-Welded Steel/Aluminum Alloy Joints with Process Tapes, *J. Mater. Eng. Perform.*, 2018, **27**(10), p 5532–5544
10. W. Zhang, D. Sun, L. Han, and Y. Li, Optimised Design of Electrode Morphology for Novel Dissimilar Resistance Spot Welding of Aluminium Alloy and Galvanised High Strength steel, *Mater. Des.*, 2015, **85**, p 461–470
11. R. Qiu, C. Iwamoto, and S. Satonaka, In Situ Scanning Electron Microscopy Observation of Fracture Crack Propagation in the Welding Interface Between Aluminium Alloy and Steel, *Mater. Sci. Technol.*, 2009, **25**(10), p 1189–1192
12. J. Chen, X. Yuan, Z. Hua, T. Li, K. Wu, and C. Li, Improvement of Resistance-Spot-Welded Joints for DP 600 Steel and A5052 Aluminum Alloy with Zn Slice Interlayer, *J. Manuf. Process.*, 2017, **30**, p 396–405
13. M.R. Arghavani, M. Movahedi, and A.H. Kokabi, Role of Zinc Layer in Resistance Spot Welding of Aluminium to Steel, *Mater. Des.*, 2016, **102**, p 106–114
14. Y. Zhang, D. Sun, H. Li, and X. Gu, Effects of Cu on Microstructures and Properties of Resistance Spot Welded Joints of Aluminum and Steel, *J. Changchun Univ. Technol.*, 2017, **38**(1), p 8–13
15. S. Rahimi and M. Movahedi, Resistance Spot Welding of Aluminum to Aluminum Clad Steel Sheet: Experimental And Theoretical Analysis, *J. Manuf. Process.*, 2020, **58**, p 429–435

16. W. Zhang, D. Sun, L. Han, and D. Liu, Interfacial Microstructure and Mechanical Property of Resistance Spot Welded Joint of High Strength Steel and Aluminium Alloy with 4047 AlSi12 Interlayer, *Mater. Des.*, 2014, **57**, p 186–194
17. H. Zhao, G. Zhang, Q. Zhang, C. Zhang, and Y. Li, Joining Mechanism and Mechanical Properties of Metallic Bump Assisted Weld-Bonded (MBaWB) Joints of AA6061-T6 and Bare DP590, *J. Manuf. Process.*, 2020, **50**, p 204–215
18. R. Qiu, N. Wang, H. Shi, L. Cui, L. Hou, and K. Zhang, Joining Steel to Aluminum Alloy by Resistance Spot Welding with a Rivet, *Int. J. Mater. Res.*, 2015, **106**(1), p 60–65
19. L. Fei, S. Zhao, P. Zhang, Z. Feng, F. Jiang, and H. Zhou, Microstructure and Mechanical Performance of Flat Resistance Element Welded Aluminum Alloy/Q235 Steel Joints, *Int. J. Adv. Manuf. Technol.*, 2022, **120**, p 6337–6349
20. G. Meschut, O. Hahn, V. Janzen, and T. Olfemann, Innovative Joining Technologies for Multi-Material Structures, *Weld. World*, 2014, **58**(1), p 65–75
21. S. Baek, G.Y. Go, J.W. Park, J. Song, H.C. Lee, S.J. Lee, S. Lee, C. Chen, M.S. Kim, and D. Kim, Microstructural and Interface Geometrical Influence on The Mechanical Fatigue Property of Aluminum/High-Strength Steel Lap Joints Using Resistance Element Welding for Lightweight Vehicles: Experimental and Computational Investigation, *J. Mater. Res. Technol.*, 2022, **17**, p 658–678
22. Y. Sun, R. Huang, H. Zhao, X. Chen, M. Jiang, L. Wu, B. Chen, and C. Tan, Enhancement of Resistance Element Welding of AA6061 to DP600 Steel by Using External Magnetic Field, *J. Manuf. Process.*, 2022, **80**, p 347–358
23. Z. Ling, Y. Li, Z. Luo, Y. Feng, and Z. Wang, Resistance Element Welding of 6061 Aluminum Alloy to Uncoated 22MnMoB Boron Steel, *Mater. Manuf. Processes*, 2016, **31**(16), p 2174–2180
24. O.Y. Hyun, R.H. Jung, K. Taejung, C. Minsu, and L. Taeseon, Mechanical Performance and Microstructure of Resistance Element Welds of Dissimilar Metals Ceated with a Headless Rivet, *Korean J. Met. Mater.*, 2019, **57**(11), p 708–714
25. X. Fang and F. Zhang, Hybrid Joining of a Modular Multi-Material Body-in-White Structure, *J. Mater. Process. Technol.*, 2020, **275**, p 116351
26. S. Niu, Y. Ma, M. Lou, C. Zhang, and Y. Li, Joint Formation Mechanism and Performance of Resistance Rivet Welding (RRW) for Aluminum Alloy and Press Hardened Steel, *J. Mater. Process. Technol.*, 2020, **286**, p 116830
27. H. Günter and G. Meschut, Joining of Ultra-High-Strength Steels Using Resistance Element Welding on Conventional Resistance Spot Welding Guns, *Weld. World*, 2021, **65**, p 1899–1914
28. S. Niu, M. Lou, Y. Ma, and Y. Li, Study on the Microstructure and Mechanical Performance for Integrated Resistance Element Welded Aluminum Alloy/Press Hardened Steel Joints, *Mater. Sci. Eng. A*, 2021, **800**, p 140329
29. C. Schmal and G. Meschut, Process Characteristics and Influences of Production-Related Disturbances in Resistance Element Welding of Hybrid Materials with Steel Cover Sheets and Polymer Core, *Weld. World*, 2020, **64**, p 437–448
30. G. Meschut, C. Schmal, and O.T. Christopher, Process Characteristics And Load-Bearing Capacities of Joints Welded with Elements the Application in Multi-Material Design, *Weld World*, 2017, **61**, p 435–442
31. J.P. Oliveira, K. Ponder, E. Brizes, T. Abke, and A.J. Ramirez, Combining Resistance Spot Welding and Friction Element Welding for Dissimilar Joining of Aluminum to High Strengths Steels, *J. Mater. Process. Technol.*, 2019, **273**, p 116192
32. M. Lou, Y. Li, Y. Wang, B. Wang, and X. Lai, Influence of Resistance Heating on Self-Piercing Riveted Dissimilarjoints of AA6061-T6 and Galvanized DP590, *J. Mater. Process. Technol.*, 2014, **214**, p 2119–2126
33. R.Y. Zhang, Y.G. He, H.X. Shi, Z.L. Zhang, and R.F. Qiu, Performance of Resistance Rivet-Welding Joint of aluminum Alloy/Low Carbon Steel, *Trans. Mater. Heat Treat.*, 2020, **41**(7), p 181–187
34. S.M. Wan, S.J. Hu, S.Y. Li, L.H. Zhang, and X.Q. Lu, Process Parameters and Joint Evaluation of self-Piercing Riveting with Half-Hollow Rivets, *J. Tianjin Univ.*, 2007, **40**(4), p 494–498
35. R. Qiu, J. Li, H. Shi, and H. Yu, Characterization of Resistance Spot Welded Joints Between Aluminum Alloy and Mild Steel with Composite Electrodes, *J. Mater. Res. Technol.*, 2023, **24**, p 1190–1202

Publisher's Note Springer Nature remains neutral with regard to jurisdictional claims in published maps and institutional affiliations.

Springer Nature or its licensor (e.g. a society or other partner) holds exclusive rights to this article under a publishing agreement with the author(s) or other rightsholder(s); author self-archiving of the accepted manuscript version of this article is solely governed by the terms of such publishing agreement and applicable law.